CILIARY INTER-MICROTUBULE BRIDGES

F. D. WARNER

Department of Biology, Biological Research Laboratories,
Syracuse University, Syracuse, New York 13210, U.S.A.

SUMMARY

Electron micrographs of both negatively contrasted and thin-sectioned lamellibranch gill cilia reveal several new features of ciliary fine structure, particularly in regard to those structures forming intermittent or permanent crossbridges between microtubules. Negative-contrasting reveals the presence of a 14·5-nm repeating bridge between the central microtubules. Frontal views of negatively contrasted dynein arm rows along subfibre A show that the arms (23-nm repeat) in the outer row are displaced in a left-handed manner by 3–4 nm with respect to those in the inner row. This displacement is probably a direct reflexion of the helical tubulin subunit lattice of the subfibre. Interdoublet (nexin) links are seen connecting adjacent A and B subfibres at intervals of 86 nm along the doublet. Negative-contrasting shows thin, highly elastic connexions holding the doublets together. When seen in longitudinal thin sections, the interdoublet links are often tilted to considerable angles, indicating they may have an elastic response to interdoublet sliding.

INTRODUCTION

The motile 9 + 2 axoneme of cilia, flagella and sperm tails is an interconnected lattice of microtubules having no fewer than 5 kinds of structures forming either intermittent or permanent crossbridges between microtubules (see Warner, 1974, for review). Studies by Summers & Gibbons (1971, 1973) and Gibbons & Gibbons (1972, 1973) have clearly shown that the generative force for flagellar motility results from active (ATP hydrolysis) crossbridge formation between adjacent doublet microtubules. The mechanochemical interaction results in sliding displacement between the doublets which is simultaneously converted into propagated bending motion.

Recently, we examined the role of the radial spokes in the sliding-bending conversion (Warner & Satir, 1974) and concluded that the spokes, in lamellibranch gill cilia, were the primary source of the internal shear resistance required to convert active interdoublet sliding into regulated, propagated bending of the organelle. Although this study presented many new details of ciliary fine structure, the observations were primarily limited to the radial spoke-central sheath complex.

Using both thin-sectioned and negatively contrasted, isolated gill cilia, it is now possible to visualize the presence of a bridge between the 2 central microtubules, to clarify the organization of the interdoublet or nexin links and to characterize the organization of the 2 rows of dynein arms along the doublet subfibre A.

MATERIALS AND METHODS

Lamellibranch gill cilia from the genus *Unio* were used in this study. For electron micro-scopy, gill tissue was isolated and fixed in 2 % glutaraldehyde adjusted to pH 7·4 with 25 mM sodium cacodylate for 1·5 h at 4 °C. Tissue was postfixed in cacodylate-buffered 1 % OsO_4 for 45 min, dehydrated in an ethanol series and embedded in Epon 812. Thin sections were stained for 15 min in 5 % aqueous uranyl acetate followed by staining for 2 min in Reynolds' lead citrate.

For some preparations, gill tissue was deciliated and the cilia purified by differential centri-fugation. Purified cilia were demembranated in Triton X-100 and either fixed as above or negatively contrasted with 2 % aqueous uranyl acetate at pH 4·5. Isolated axonemes are functionally intact; that is, they will reactivate and beat normally upon the addition of ATP. Details of the isolation, purification and reactivation procedure will be published in a future paper.

OBSERVATIONS AND DISCUSSION

The movement of axonemal microtubules during ciliary or flagellar beating must be regarded as a very dynamic process, since each doublet microtubule slides with respect to every other doublet and with respect to the central microtubule complex, even though the major part of this sliding may be only a passive response to the active sliding generated between any 2 doublets at a particular instant during the beat cycle. Since we know that each linear element moves with respect to all other linear elements (Warner, 1972; Warner & Satir, 1974), all structural crossbridges between micro-tubules, whether intermittent or permanent, must be brought into the conceptual framework of the sliding filament model of ciliary motility (Satir, 1968).

Central microtubule bridge

Lamellibranch gill cilia have a prominent 'bridge' which occurs between doublet numbers 5 and 6 and forms the main morphological marker for determining orienta-tion of the cilium (Gibbons, 1961; Satir, 1965, 1968). The bridge appears to be a manifestation of arm structure between these doublets, that is, the arms of both rows of doublet 5 appear to be permanently crossbridged to doublet 6. The bridge is readily apparent in transversely sectioned cilia (Figs. 1, 11–14) and individual elements repeat at 23 nm along the A subfibre (Warner & Satir, 1974).

Our previous study of lamellibranch gill cilia (Warner & Satir, 1974) described in detail the organization of the central sheath-microtubule complex. The sheath con-sists of paired rows of projections along each of the 2 central microtubules to which are attached, intermittently, the radial spoke heads. Longitudinal thin sections suggested the presence of a periodic bridge between the central tubules (as have numerous other studies, e.g. Gibbons, 1961) but superimposition of the sheath projection rows could also account for the bridged appearance, particularly since the measured periodicity is the same for both projections and the bridge region.

When seen in transverse sections, the central sheath projections, although not clearly resolved, form a circular profile around the central tubules (Fig. 1) and there also appears to be material or a bridge joining the 2 tubules at the axoneme axis. This bridge spans the 8-nm space between tubules and often appears to be double. How-

ever, a straightforward answer regarding the presence of a central microtubule bridge is provided by negatively contrasted images of the central complex.

Fig. 2 shows an intact central tubule-sheath complex and again it is not possible to separate the image of the sheath projections from the bridge region. Fig. 3 shows a central pair with most of the sheath material solubilized except that along 1 tubule, a single doublet remains attached to the sheath via the triplet radial spokes. Fig. 4 shows a central pair with all sheath material removed: clearly there remains a prominent 14·5-nm repeating bridge between the 2 tubules. Fig. 5 shows a similar preparation except that the central pair has pulled apart and the bridge elements remain attached to only one of the tubules. Although it appears from these preparations that only a single row of bridge elements occurs between the central tubules, the same arguments that apply to possible dynein arm superimposition (see next section) also apply here.

Dynein arm organization

All motile 9 + 2 cilia, flagella and spermtails have an ATPase, dynein, located in the 2 orderly rows of arms of subfibre A of each doublet microtubule. The dynein arms are the principal and probably sole source of mechanochemical interaction which results in doublet sliding (Summers & Gibbons, 1971, 1973). This mechanochemical activity was beautifully demonstrated by Gibbons & Gibbons (1973) when they selectively solubilized only the 9 outer rows of arms and observed, in ATP-reactivated flagella, that the axonemes then beat with precisely one-half the frequency of untreated control flagella.

The precise organization and periodicity of the dynein arms along a given doublet has remained uncertain, mainly because it is difficult both to preserve and to distinguish between the 2 rows when seen in longitudinal thin sections, and negative-contrasting usually results in their solubilization. The reported periodicity of arms along a doublet spans a considerable range (12–24 nm), which has caused Chasey (1972) to suggest that the arms of 1 row may be half-staggered with respect to those in the other row. Thus the 12–24 nm range could be easily accounted for, if in some instances both rows had been seen superimposed while in other instances they had been seen individually.

Both negatively contrasted and thin-sectioned arm rows are seen in Figs. 6 and 15. The arms repeat at 23 nm, centre-to-centre along the subfibre. Although the possibility of superimposition of the 2 adjacent rows cannot be ruled out in images such as Fig. 6, it appears that only a single row is represented. To test for superimposition artifact, and to provide a straightforward answer as to arm period and inter-row relationships, frontal views of the arms are required; that is, both rows of arms along a single doublet subfibre A need to be viewed from the position of the opposing B subfibre. Figs. 7 and 8 show frontal views of the dynein arm rows from doublets at the edges of negatively contrasted, demembranated but structurally intact cilia similar to Fig. 6. Two rows can be seen along each doublet and the arm periodicity in each row is 23 nm centre-to-centre. Occasionally the arm rows have an obvious scalloped appearance (Fig. 9), which probably results from overlying regions of incompletely solubilized membrane. It is apparent in Figs. 7 and 8 that the 2 rows are slightly

displaced, that is, the arms in one row are not in lateral register with those of the other row. Although precise measurement is difficult, the arms in the outer row appear to be displaced in a left-handed manner by 3–4 nm (10 degrees) with respect to their immediate neighbour in the inner row. The 2 rows are separated by 15–16 nm. This displacement is consistent with the helical displacement of tubulin subunits found in the A subfibre by Amos & Klug (1974). It is reasonable to think that the arms are precisely positioned on the A subfibre with respect to one of the helical families of the tubulin subunit lattice. The observed arm displacement matches most favourably with the 3-start, left-handed family, assuming that 2–3 protofilaments lie between the 2 rows of arms. However, optical diffraction data are necessary to match precisely the arm array with the tubulin helix.

The high frequency of appearance of the double rows of arms (sometimes seen on both sides of the same axoneme) eliminates the possibility of the image representing only the doublets 5–6 bridge. Although usually the arms are not visible on fragmented doublet microtubules, occasionally a prominent 23-nm repeat can be seen which is probably related to one of the rows (Fig. 10).

Interdoublet link organization

Thin connexions, termed interdoublet, nexin or circumferential links (for review see Stephens, 1974; Warner, 1974) are often seen in cross-sections of cilia and flagella. The links lie near the centrifugal side of the inner dynein arms and extend about 18 nm to the adjacent B subfibre (Figs. 11–14). The visibility of the links is enhanced in demembranated axonemes, presumably because of the loss of non-structural matrix material from the organelle (e.g. compare Figs. 11 and 12). The frequency of appearance of the links in a given ciliary cross-section is low ($\sim$ 2–4, Figs. 11, 13; Fig. 12 is exceptional), suggesting that their periodicity along the doublet is in the range of typical section thickness (70–100 nm). The inter-doublet links should not be confused with similar but structurally prominent connexions between doublet microtubules that are restricted to the region immediately distal to the basal plate of some cilia and flagella (e.g., *Chlamydomonas* flagella; Witman, Carlson, Berliner & Rosenbaum, 1972).

Stephens (1970) attempted an initial characterization of the interdoublet link material in *Arbacia* sperm flagella and termed the isolated protein nexin. His thermally fractionated preparations consisted largely of A subfibres to which adhered clumps of material repeating at about 100 nm along the subfibre. When negatively stained, this clumped material seemed to hold adjacent A subfibres together on the carbon supporting film, and Stephens concluded that the material, nexin, joined adjacent A subfibres in the native organelle, rather than joining A to B. Similar interpretations have been made on sectioned cilia (Linck, 1973 a, b) although the published micrographs generally do not substantiate that conclusion.

In the present study, cross-sections of isolated, demembranated cilia indicate that the interdoublet link joins A subfibres to adjacent B subfibres, and similar images appear in numerous other studies (e.g. Gibbons & Fronk, 1972; Gibbons & Gibbons, 1973; Linck, 1973 a, b). Furthermore, when the links are occasionally seen in

longitudinal sections (Fig. 15), they still appear to join A to B. The apparent conflict between Stephens' (1970, 1971, 1974) observations and the present study (species differences seem unlikely) can probably be resolved by analysis of radial spoke grouping along the A subfibre. Negatively contrasted preparations of collapsed gill cilia clearly reveal the 86-nm repeat triplet grouping of the radial spokes (Figs. 3, 16). The spokes, however, are often collapsed together into repeating clumps of material along the A subfibre (Fig. 16). The spokes appear to hold the doublets firmly together on the carbon supporting film, which suggests that the spoke material is 'sticky' and has some affinity (probably artifactual) for other axoneme components or microtubules.

At the time of Stephen's (1970) study, it was not generally known that the radial spokes were a major axonemal component and it is possible that the nexin links were in fact groups of clumped radial spokes. His micrographs of negatively contrasted A subfibre nexin links (Stephens, 1971) strongly resemble the spoke groups in Fig. 16, and do not resemble the thin connexions observed in this study (see below).

Negatively contrasted gill cilia occasionally show thin connexions joining the A and B subfibres of adjacent doublets (Fig. 17). These thin links are somewhat irregular in periodicity, but the smallest separation measured is about 50 nm, while the largest is about 100 nm. It is obvious that the connexion has stretched considerably and in some preparations the links may span as much as 300 nm between doublets. Similar connexions were seen by Linck (1973 b) in negatively contrasted *Aequipecten* gill cilia. However, it should be cautioned that the thin connexions visible in Fig. 17 cannot be unequivocally identified as the interdoublet links appearing in thin sections (Figs. 11–15).

Recently, Dallai, Bernini & Giusti (1973) described interdoublet connexions in the axonemes of *Sciara* sperm flagella, which do not have the usual 9+2 organization. In thin sections, the links clearly join adjacent A and B doublet subfibres in a position similar to that occurring in 9+2 cilia and flagella. When negatively contrasted, the links appear as a thin connexion between subfibres with a regular repeat of about 90 nm. These links are also very elastic, often spanning 200–300 nm separations between doublets. It remains to be determined if these connexions are homologous to the interdoublet links of 9+2 axonemes.

When the interdoublet links are seen in longitudinal thin sections, their periodicity is more regular, typically lying at about 86-nm intervals along the doublet (Fig. 15). The links are only visible in the region where the section plane appears to pass between the inner and outer rows of dynein arms and they usually lie at angles other than 90° to the A subfibre (see below).

Previous discussions of the interdoublet links (Warner, 1974; Warner & Satir, 1974) indicated that, like any connexions between sliding microtubules, the links must be capable of some manner of displacement in order to permit interdoublet sliding. Two possible mechanisms for this displacement exist: (1) the links function as part of a mechanochemical event, perhaps interacting with the inner row of dynein arms; or (2) the links are inherently elastic and thus capable of considerable angular displacement, which must be at least as great as the maximum relative movement between adjacent doublets. No evidence exists in support of the first contention and little can

be said except that mechanochemical activity of these structures would substantially increase the complexity and coordination of known mechanochemical events related to the sliding-bending mechanism.

Certain evidence supports the idea that the links may be inherently elastic, apart from the observation of extensive stretching of intermicrotubule connexions in negatively contrasted preparations (Fig. 17; Dallai *et al.* 1973; Linck, 1973*b*). Fig. 15 shows several interdoublet links in longitudinal section of a cilium. The links are uniformly tilted to an angle of about 45° from the perpendicular. Since the normal (interdoublet sliding absent) orientation of the links appears to be perpendicular to the doublet, it appears that some interdoublet displacement and concomitant link extension is visible in this particular cilium. Knowing the distance separating adjacent A and B subfibres (18 nm) and the link angle (45°), it is possible to calculate from simple geometrical expressions (Warner, 1972; Warner & Satir, 1974), both the amount of interdoublet sliding that has occurred and the necessary link extension to accommodate this sliding. For Fig. 15, the displacement is about 18 nm, requiring a total link length of about 25·5 nm, which is an approximate 41 % increase. Maximum predicted interdoublet sliding (doublets 3-4, 7-8) is about 30 nm for a cilium with a bend angle of 100°, requiring an approximate 90 % increase in the length and a maximum tilt angle of 60° of the interdoublet connexions. Several images similar to Fig. 15 have been obtained with maximum link angles of about 55°, which strongly supports the notion that the links are permanently bridged and inherently elastic and thus capable of significant angular displacement in response to interdoublet sliding.

The function of the interdoublet links in the motile mechanism must, for the time being, remain speculative. Are they an elastic force providing shear resistance and thus related directly to the sliding-bending conversion, or do they simply represent a component which contributes to the maintenance of geometrical positioning within the axoneme? Summers & Gibbons (1971, 1973) briefly treated isolated sperm flagella with trypsin, resulting in partial proteolytic disruption of both the interdoublet links and the radial spokes. The flagella then lost the capacity to beat normally upon the addition of ATP but retained the capacity for active interdoublet sliding. Similar results have been obtained with isolated gill cilia (Warner, unpublished results). Clearly then, one or both of these linkage components function during bending, although data from Warner & Satir (1974) indicate that radial spoke activity is the primary event associated with the conversion of active sliding into regulated bending.

REFERENCES

AMOS, L. A. & KLUG, A. (1974). Arrangement of subunits in flagellar microtubules. *J. Cell Sci.* **14**, 523–549.

CHASEY, D. (1972). Further observations on the cilia of *Tetrahymena pyriformis. Expl Cell Res.* **74**, 471–479.

DALLAI, R., BERNINI, F. & GIUSTI, F. (1973). Interdoublet connections in the sperm flagellar complex of *Sciara. J. submicrosc. Cytol.* **5**, 137–145.

GIBBONS, B. H. & GIBBONS, I. R. (1972). Flagellar movement and adenosine triphosphatase activity in sea urchin sperm extracted with Triton X-100. *J. Cell Biol.* **54**, 75–97.

GIBBONS, B. H. & GIBBONS, I. R. (1973). The effect of partial extraction of dynein arms on the movement of reactivated sea-urchin sperm. *J. Cell Sci.* **13**, 337–357.

GIBBONS, I. R. (1961). The relationship between the fine structure and direction of beat in gill cilia of a lamellibranch mollusc. *J. biophys. biochem. Cytol.* **11**, 179–205.

GIBBONS, I. R. & FRONK, E. (1972). Some properties of bound and soluble dynein from sea urchin sperm flagella. *J. Cell Biol.* **54**, 365–381.

LINCK, R. W. (1973a). Comparative isolation of cilia and flagella from the lamellibranch mollusc, *Aequipecten irradians. J. Cell Sci.* **12**, 345–367.

LINCK, R. W. (1973b). Chemical and structural differences between cilia and flagella from the lamellibranch mollusc, *Aequipecten irradians. J. Cell Sci.* **12**, 951–981.

SATIR, P. (1965). Studies on cilia. II. Examination of the distal region of the ciliary shaft and the role of the filaments in motility. *J. Cell Biol.* **26**, 805–834.

SATIR, P. (1968). Studies on cilia. III. Further studies on the cilium tip and a 'sliding filament' model of ciliary motility. *J. Cell Biol.* **39**, 77–94.

STEPHENS, R. E. (1970). Isolation of nexin – the linkage protein responsible for the maintenance of the nine-fold configuration of flagellar axonemes. *Biol. Bull. mar. biol. Lab., Woods Hole* **139**, 438.

STEPHENS, R. E. (1971). Microtubules. In *Biological Macromolecules*, vol. 5 (ed. S. N. Timasheff & G. D. Fasman), pp. 355–391. New York: Marcel Dekker.

STEPHENS, R. E. (1974). Enzymatic and structural proteins of the axoneme. In *Cilia and Flagella* (ed. M. A. Sleigh), pp. 39–76. London: Academic Press.

SUMMERS, K. E. & GIBBONS, I. R. (1971). Adenosine triphosphate-induced sliding of tubules in trypsin-treated flagella of sea urchin sperm. *Proc. natn. Acad. Sci. U.S.A.* **68**, 3092–3096.

SUMMERS, K. E. & GIBBONS, I. R. (1973). Effects of trypsin digestion on flagellar structures and their relationship to motility. *J. Cell Biol.* **58**, 618–629.

WARNER, F. D. (1972). Macromolecular organization of eukaryotic cilia and flagella. In *Advances in Cell and Molecular Biology*, vol. 2 (ed. E. J. Du Praw), pp. 192–235. New York: Academic Press.

WARNER, F. D. (1974). The fine structure of the ciliary and flagellar axoneme. In *Cilia and Flagella* (ed. M. A. Sleigh), pp. 11–37. London: Academic Press.

WARNER, F. D. & SATIR, P. (1974). The structural basis of ciliary bend formation. Radial spoke positional changes accompanying microtubule sliding. *J. Cell Biol.* **63**, 35–63.

WITMAN, G. B., CARLSON, K., BERLINER, J. & ROSENBAUM, J. L. (1972). *Chlamydomonas* flagella. I. Isolation and electrophoretic analysis of microtubules, matrix, membranes, and mastigonemes. *J. Cell Biol.* **54**, 507–539.

All figures (except Fig. 15) are at a magnification of × 180 000.

Fig. 1. Transverse section of an isolated, demembranated cilium showing an apparent bridge between the 2 central microtubules (arrows). The central tubule-sheath complex on the right (*cm*) has become separated from the remainder of the axoneme. *b*, doublets 5–6 bridge.

Fig. 2. Uranyl acetate negatively contrasted central microtubule-sheath complex. The overlying sheath projections obscure the bridge region between the 2 tubules.

Fig. 3. Central microtubule-sheath complex (*cm*) to which a single doublet (*a*, *b*) remains attached via the 86-nm repeating groups of triplet radial spokes (brackets). Most of the sheath projections have been solubilized, but because of the plane of tubule collapse, the bridge region is not clear.

Fig. 4. Central pair microtubules from which all sheath material has been solubilized. The 2 tubules remain held together by the bridge projections repeating at 14·5 nm (arrows).

Fig. 5. Central pair microtubules from which all sheath material has been solubilized. The 2 microtubules have separated but the bridge projections remain attached to one of the tubules (arrows).
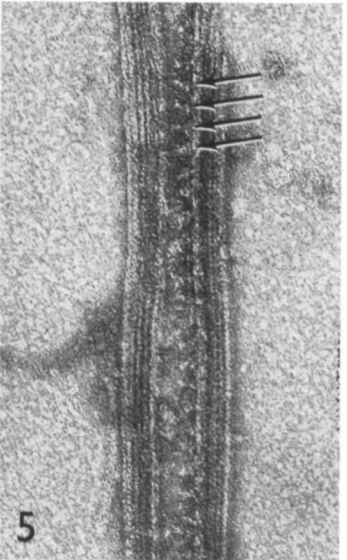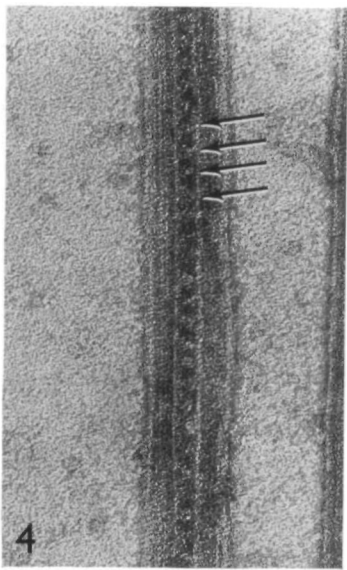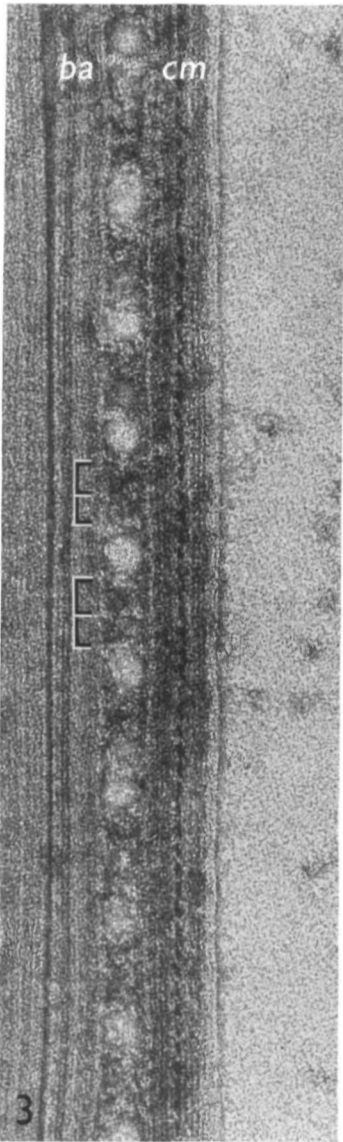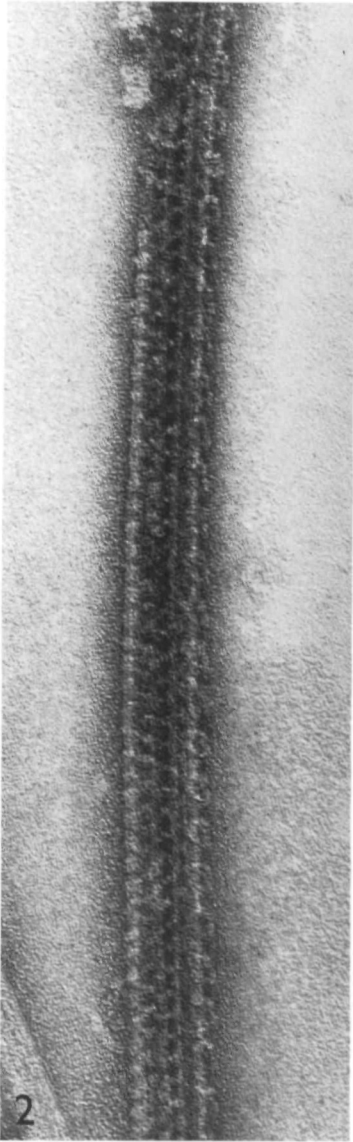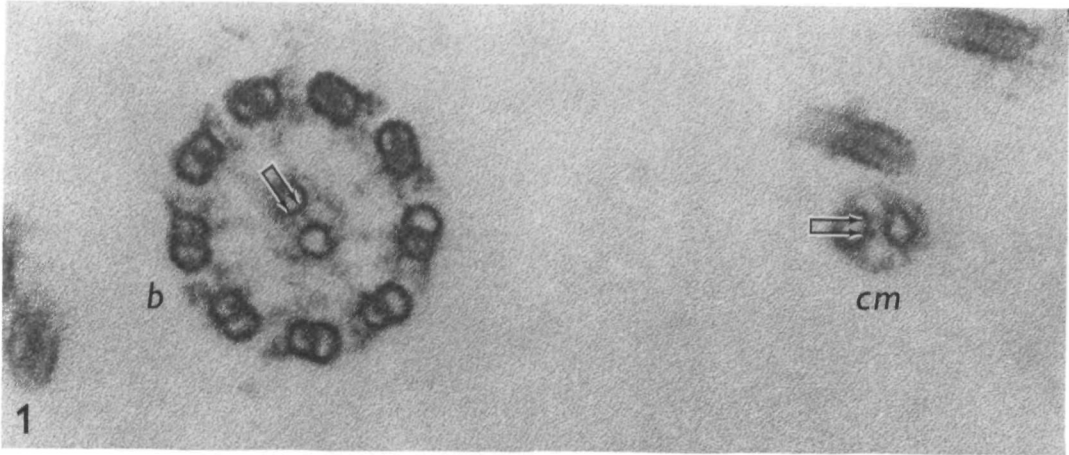
Fig. 6. Uranyl acetate negatively contrasted, intact but demembranated cilium. Single rows of dynein arms repeating at 23 nm are visible at both sides of the axoneme (arrows).

Figs. 7, 8. Frontal views of subfibre A from a doublet at the edge of an intact cilium. Both the inner (*i*) and outer (*o*) arm rows are visible: the arms repeat at 23 nm in both rows. Arms of the outer row appear to be displaced by 3–4 nm in a left-handed manner with respect to the arms in the inner row (lines).

Fig. 9. Frontal view of a doublet where it appears that incompletely solubilized membrane has collapsed over the arm rows resulting in a characteristic scalloped appearance (arrows). The scallop repeat is 23 nm.

Fig. 10. Fragmented doublet microtubule showing a prominent 23-nm repeat (arrows) that is probably related to one of the arm rows. The repeat appears to be contrasted in the cleft between the 2 subfibres of the doublet.

F. D. Warner
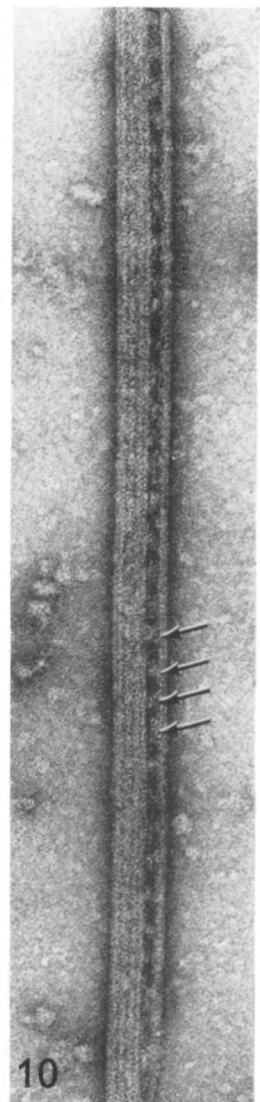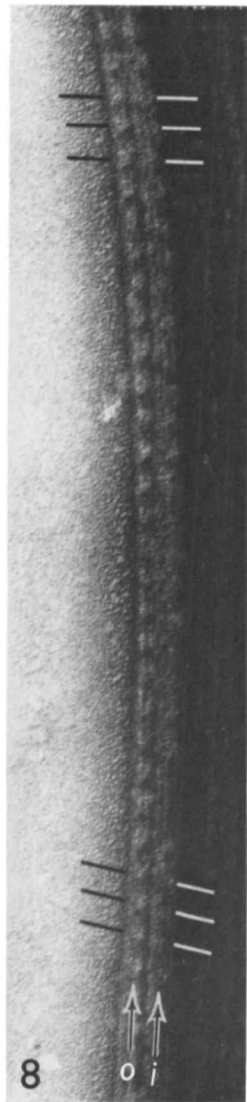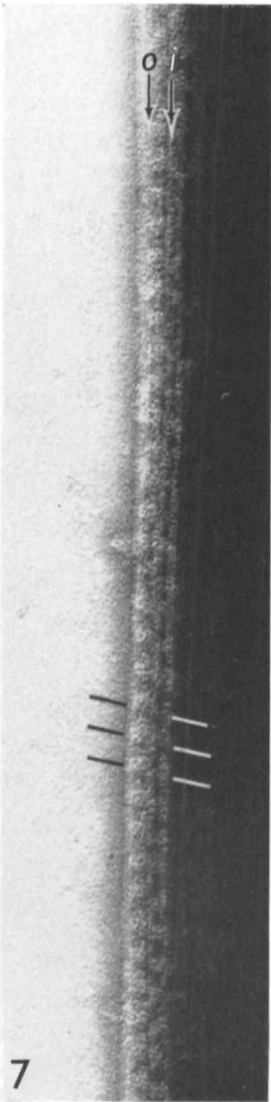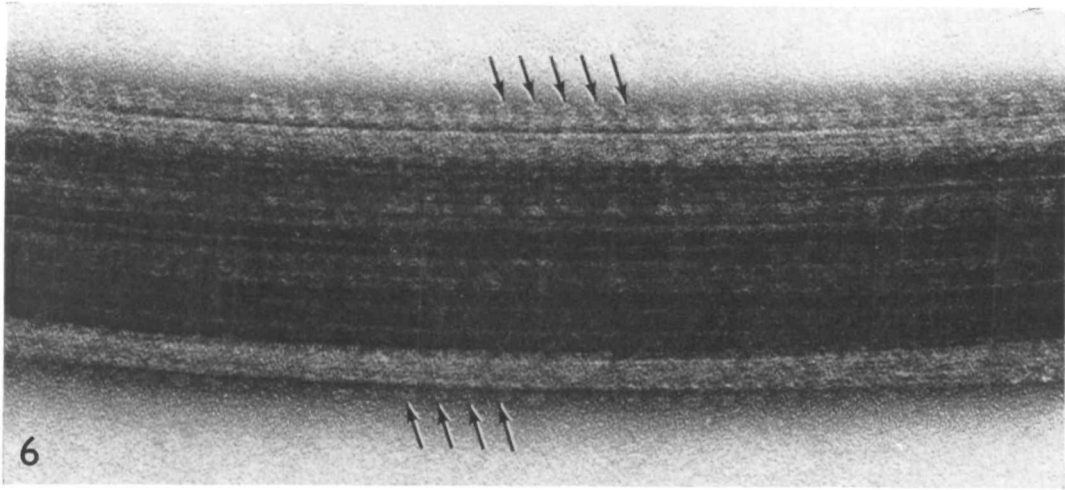
Fig. 11. *In situ* cilium seen in transverse section. Interdoublet links (arrows) connect adjacent A and B subfibres in the region of the inner dynein arms. The direction of view is from cilium base-to-tip with the doublets 5–6 bridge (*b*) located in the 6 o'clock position.

Figs. 12–14. Isolated, demembranated cilia seen in varying degrees of disassociation. Interdoublet links can be seen in all cilia but are particularly clear in Fig. 12. Cilium orientation and bridge (*b*) position is the same as in Fig. 11.

Fig. 15. Longitudinal section in the region of 3 adjacent doublets of an *in situ* cilium. Dynein arms are visible along 2 of the doublets (arrows). Several interdoublet links (lines) can be seen connecting adjacent *a* and *b* subfibres. The links repeat at 86 nm along the subfibres and are positioned at an angle of about 45° from the perpendicular, indicating that some sliding displacement has occurred between the 2 doublets. × 160 000.
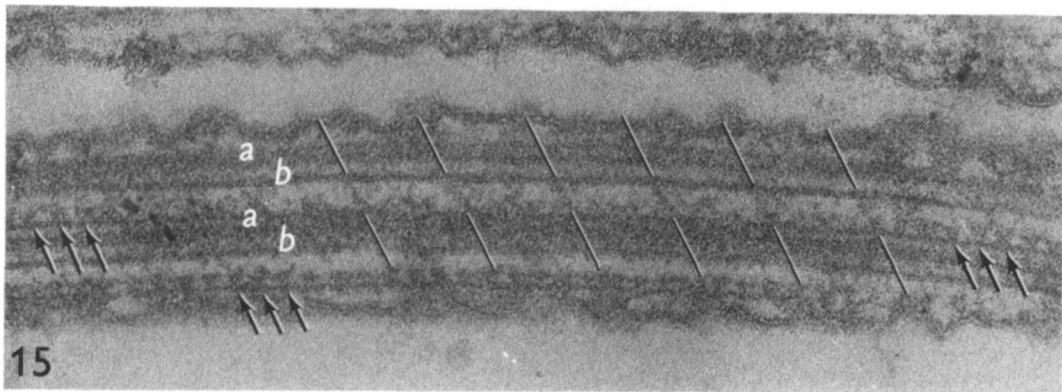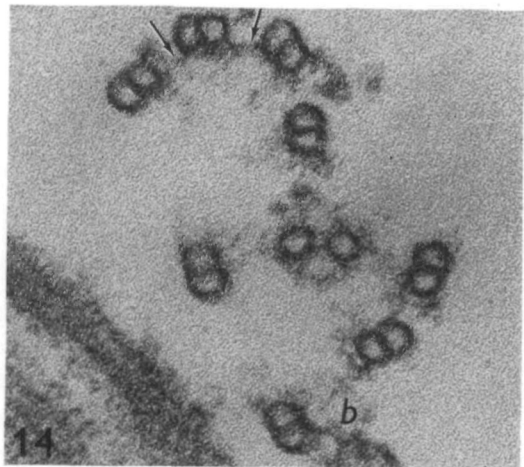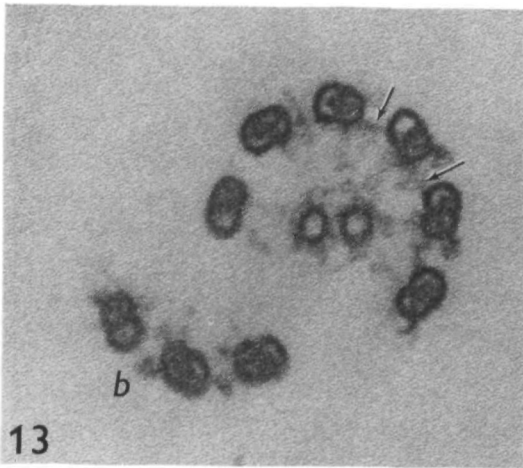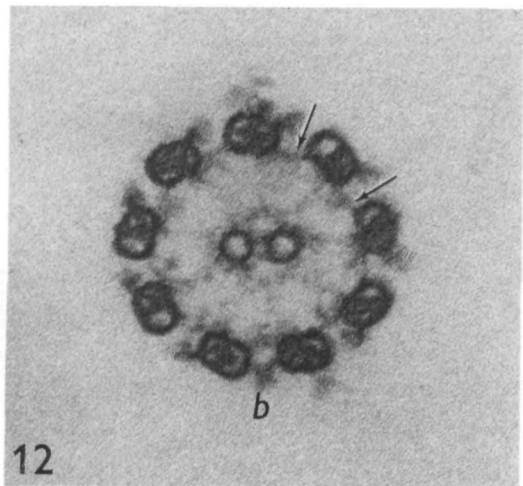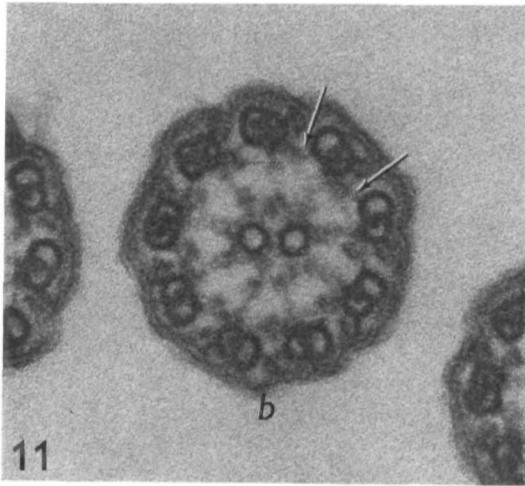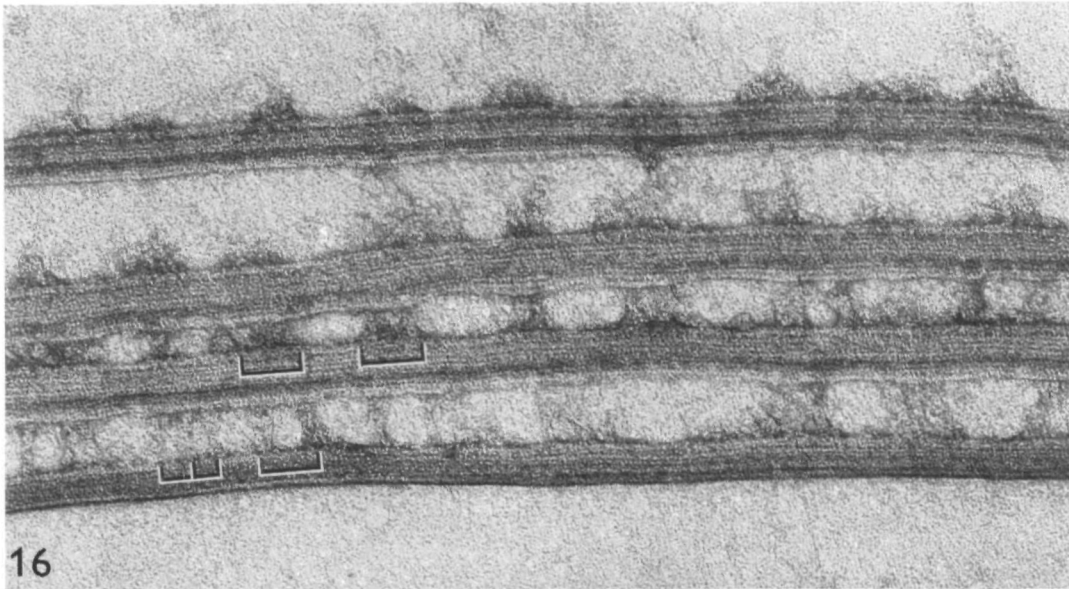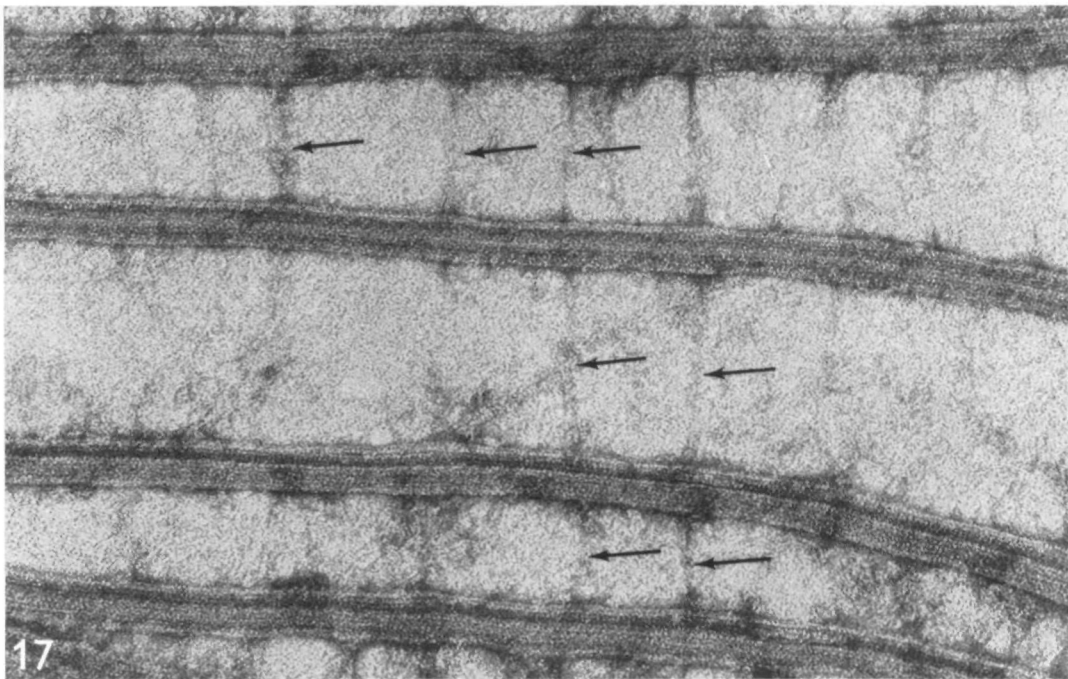
Fig. 16. Uranyl acetate negatively contrasted doublet microtubules. The groups of triplet radial spokes (brackets) repeat at 86 nm along the doublet and often are clumped together so that individual spokes are not resolved. The spoke groups appear to be holding the doublets together on the carbon support film although this is an artifactual condition that occurred during collapse and staining of the axoneme.

Fig. 17. Several doublets from a single cilium which show thin connexions (arrows) with a 50–100 nm repeat between the doublets. The links appear to have stretched considerably since doublet separation is about 150 nm. Spoke groups have apparently been solubilized from these 4 doublets (subfibre A is at the top of each) but were visible in the remaining doublets similar to Fig. 16.